Korean J. Chem. Eng., 37(6), 985-999 (2020)
DOI: 10.1007/s11814-020-0526-1

pISSN: 0256-1115
eISSN: 1975-7220

Highly efficient removal from aqueous solution by adsorption of Maxilon Red GRL dye using activated pine sawdust

İlknur Şentürk*,† and Muhammed Reha Yıldız**

*Department of Environmental Engineering, Engineering Faculty, Sivas Cumhuriyet University, Sivas, 58140, Turkey
**Department of Environmental Engineering, Graduate School of Sciences, Sivas Cumhuriyet University, Sivas, 58140, Turkey
(*Received 4 January 2020 • accepted 27 February 2020*)

Abstract−Pine sawdust, to which sulfuric acid was applied (APSD), was utilized as an inexpensive adsorbent to perform the batch adsorptive removal from a synthetic dye solution of Maxilon Red GRL (MR GRL). The activated adsorbent was characterized by the points of zero charge, FTIR, N_2 adsorption-desorption, SEM, and SEM-EDX analyses. According to the removal results, the highest efficiency of the dye adsorption was reached at 180 min. MR GRL removal of 99.35% was achieved using APSD under the optimum conditions (pH=5.7-6.0, temperature=298 K, dye concentration=250 mg/L, and adsorbent dosage=8 g/L). The Langmuir isotherm represents the best explanation model for the experimental data, which has the highest adsorption capacity of 312.5 mg/g at 318 K. The compatibility of adsorption with the Langmuir isotherm showed that adsorption was reversible and physical. The other results obtained confirmed this situation. The kinetic research demonstrated that the sorption process was realized in accordance with the pseudo-second-order kinetic model. The thermodynamic parameters revealed that the MR GRL adsorption occurred spontaneously and was exothermic. The findings of the present research confirm that acid-activated pine sawdust may be utilized to remove MR GRL dye from aqueous solutions as a low-cost and efficient adsorbent.

Keywords: Maxilon Red GRL Adsorption, Chemical Activation, Pine Sawdust, Kinetic and Thermodynamic

INTRODUCTION

According to the latest data, there are more than 100,000 commercial dyes [1]. It has been estimated that over 700,000 tons of dyes are being produced annually and about 350,000 tons are wasted every year during the different stages of manufacturing and in textile dyeing [2]. Basically, the exact data on the amount of dyes discharged from various processes in the environment are unfortunately unknown [1]. During the production of textile products, large amounts of water are consumed, especially by dyeing and printing processes. A textile avian with a daily production capacity of 8,000 kg has a daily water consumption of nearly 1.6 million liters. Nearly 25% of whole of water consumption is required for dyeing and printing processes. According to the US EPA, 40 liters of water is required averagely for dyeing 1 kg of cloth, changing according to the textile material and dyeing process. Water is also required for other processes, such as washing of dyed textile material [3]. Most dyes are difficult to decolorize due to their complex structure and synthetic origin as they are designed to resist fading upon exposure to different factors as light, water, and oxidizing agents and as such are very stable and difficult to degrade [4].

The textile industry is the largest user of synthetic dyes. Therefore, textile wastewater has a high pollutant content due to chemical dyes, acid or corrosive substances, dissolved solids, toxic compounds, natural impurities extracted from the product processed as a raw material (natural and synthetic fibers), and intense color. Approximately 8-20% unutilized dyes and auxiliary chemicals are discharged into the environment as textile effluent from textile industries. Thus, tons of dyes are discharged daily into the environment as aquatic waste. Even the presence of a small quantity of these compounds (less than 1 ppm) in water has adverse effects [5]. The discharge of these wastewaters to the environment leads to aesthetic issues because of the color they contain and impairs the quality of the receiving water because most of the dyes released to the environment and their decomposition products have carcinogenic and mutagenic effects on aquatic life due to their high toxicity [6-8].

Azo dyes (60-70%), a dye group commonly utilized in the textile industry, are used in dyeing cotton, royan, wool, silk, leather, and nylon. Azo dyes contain one or more azo groups (R1-N=N-R2) with polyaromatic rings, which are often replaced by sulfonate groups. Due to their complex aromatic conjugated structure, azo dyes give an intense color, have high solubility in water, and are resistant to degradation under normal conditions [9,10]. Furthermore, the wide use of this group of dyes shows that most of their reaction products, including aromatic amines, exhibit a highly carcinogenic effect. Thus, the removal and determination of these dyes prior to discharge into wastewater is of primary importance for the environment [11]. One of the most frequently utilized synthetic azo dyes for textile dyeing is Maxilon Red GRL. MR GRL is utilized as a model compound of azo dyes, representing more than half of the manufacturing of dyes on a global scale. The mentioned dyes are among the most problematic dyes in industrial wastewaters, which are frequently used for textile dyeing [11].

Currently, different technologies are accessible to decrease the

†To whom correspondence should be addressed.
E-mail: ilknurg.senturk@gmail.com, ilknursenturk@cumhuriyet.edu.tr
Copyright by The Korean Institute of Chemical Engineers.

absorption of these dyes into the environment such as ion exchange, coagulation-flocculation, chemical sedimentation, electrochemical reduction, chemical oxidation, advanced oxidation processes, membrane separation, aerobic/anaerobic microbial degradation and adsorption [1,5,13]. Most conventional wastewater treatment methods are insufficient in the treatment of such dyes and their by-products since dyes are highly resistant to heat, light, and microbial attacks because of their synthetic origin and complex aromatic molecular structure [14,15]. The advantages and disadvantages of different dye removal methods are shown by Yagub et al. [1,16]. In developing countries, these methods are still too expensive to be widely used. Therefore, researchers are investigating more environmental and effective alternative treatment methods.

Among these methods, adsorption technology and applications in wastewater treatment are receiving more and more attention [13]. Adsorption onto raw and modified materials is one of the most effective processes of advanced wastewater treatment due to the lack of hazardous by-product formation, simple design, ease of use, eco-friendliness, economical for the decontamination of dye-loaded effluents, insensitivity to toxic substances, the capability to treat dyes in more concentrated forms, more efficient in comparison with other methods, and its flexibility under operating conditions [17].

Many researchers have been working on the usage of inexpensive or no-cost industrial and agricultural wastes as adsorbents for purification of wastewater containing dyes [7]. Agricultural wastes, especially leaves and wooden debris, have been pointed out as promising materials for industrial wastewater treatment thanks to their insignificant cost, abundance, and renewability and especially their important outer and inner surface as well as the presence of various functional groups leading to the fixation of dye molecules. Sawdust, preferred as the adsorbent in this study, is a highly promising agricultural waste material used to remove undesired dyes and other pollutants from water. Activating this waste material by chemical addition increases the efficiency even more.

As a natural waste biomass, sawdust is produced in an abundant amount, especially by industrial, agriculture and forestry activities. Sawdust has various significant advantages, such as quantity, cost, ready availability, effective sorbent, biodegradability, and renewability. Sawdust is mostly composed of cellulose, hemicellulose, and lignin. Also it includes some functional groups (e.g., carboxyl, phenolic, hydroxyl, etc.) in its structure that make sorption achievable. All the mentioned characteristics turn sawdust into an efficient adsorbent that can adsorb many types of pollutants and is suitable for adsorption [18,19]. The studies demonstrate that sawdust is one of the most promising adsorbents among low-cost adsorbents to remove various types of dyes and some other unwanted materials from aquatic solutions. Hence, interest in the usage of sawdust as an adsorbent has recently increased [18,20-24]. The sawdust is good alternative for removing dyes from the aqueous solution due to their natural abundance and their low costs, when compared with other adsorbents such as activated carbon [25]. Ferrero [26] and Hamdaoui [27] showed that wood sawdust is a promising low-cost material for the treatment of polluted water containing cationic dyes since it has a high adsorption capacity compared with other agro industrial wastes [28].

On the other hand, recent studies have demonstrated that activating this waste material by chemical addition increases their dye removal efficiency even more. This chemical treatment includes the use of various acids, bases, and salts. It not only positively impacts the physical aspect of the used material, making it more porous and kinky, but also boosts the appearance of new functional groups on its surface by shifting the atomic arrangement of the lignin and cellulose matrix into a more stable structure [29-31]. In this context, our previous study proved also that acid-modified pistachio shell could be considered as an attractive low-cost agricultural by-product for the removal of dyes from synthetic aqueous solutions in batch mode, with adsorption capacity of AV 17 about 26.455 mg/g [32].

However, as we have seen in our literature review, no studies have been performed to date using chemical-pretreated pine sawdust for the adsorption removal of MR GRL dye. In this study, in which MR GRL was selected as the target pollutant due to its toxic properties and sawdust was selected as an adsorbent because of its high adsorption ability. Afterward, the removal of MR GRL dye from the aquatic environment by adsorption on acid-treated pine sawdust was examined. Then, the impacts of different operating parameters, such as contact time, adsorbent dosage, initial solution pH, initial dye concentration, solution temperature, and ionic strength, on adsorption were examined. Detailed kinetic and isotherm studies were performed to characterize adsorption. Ritchie's-second-order, pseudo-second-order, Weber-Morris, and Elovich kinetic models were utilized for the purpose of testing the adsorption kinetic data, whereas the Langmuir, Freundlich, Temkin, Dubinin-Radushkevich (D-R), and Redlich-Peterson (R-P) isotherm models were employed for the analysis of the equilibrium data.

EXPERIMENTAL

1. Adsorbent

Natural pine sawdust was acquired from a local source in Sivas, Turkey. It was first washed thoroughly with deionized water for the removal of dust and other impurities, then was dried in an oven at 80 °C until achieving a constant weight. The sawdust was ground and sieved to a particle size ranging between −0.38 and +2 mm (USA standard mesh opening). The acquired material was called raw pine sawdust (PSD) and stored in a brown glass bottle. Besides the raw pine sawdust, the impact of pretreatment on the adsorption capacity of the adsorbent was assessed by studying the raw pine sawdust sample pretreated with acid (H_2SO_4) and base (NaOH). Lower environmental load in its life cycle, less corrosive ability and economic feasibility are the major merits of selecting NaOH and H_2SO_4 as a modifying agent.

1-1. Pretreatment with H_2SO_4

200 ml of the prepared 1 N H_2SO_4 solution and 20 g of raw pine sawdust were transferred to a flask of 500 ml and mixed. Afterward, the mixture was heated in a muffle oven at 150 °C for a period of 24 h. The heated material was washed using distilled water and immersed in a 1% sodium bicarbonate solution for a night for the removal of residual acid [23]. Following the above-mentioned reaction, the solid phase was separated as a result of filtration, then washed using distilled water a number of times to remove all excessive modi-

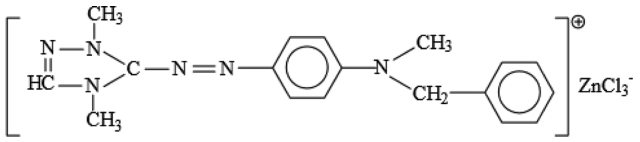

Fig. 1. Structure of MR GRL dye.

fication agents and dried, as stated earlier. The final product acquired was kept in a brown glass bottle for further use. The resulting material was named pine sawdust treated with sulfuric acid (APSD).

1-2. Pretreatment with NaOH

50 ml of the prepared 0.25 N NaOH solution and 1 g of raw pine sawdust were mixed in a 250 ml flask. Afterward, the mixture was stirred at 300 rpm/min at room temperature for a period of 1 h. Deionized water was used to wash the mixture a few times for the removal of excessive NaOH, following which it was dried for a night in an oven at a temperature of 60 °C [33]. The final product acquired was kept in a brown glass bottle for further use. The resulting material was named pine sawdust treated with sodium hydroxide (BPSD).

2. Adsorbate

The cationic azo dye Maxilon Red GRL, which was supplied from a textile factory in Kayseri, Turkey, and had a commercial quality, was utilized without further purification. The MR GRL stock solution was prepared as a result of dissolving 1 g of MR GRL in 1 liter of distilled water. The stock solution was diluted in accurate proportions for the purpose of producing solutions of different initial concentrations. The remaining chemicals utilized were of analytical grade. The chemical structure of the dye is shown in Fig. 1.

3. Instruments and Analysis Method

A scanning electron microscope (SEM, Tescan Mira3 XMU) was utilized to determine the morphological properties and surface features of the adsorbent. Fourier transform infrared spectroscopy (FTIR, Bruker Tensor II) was utilized to identify functional groups on the adsorbent. The specific surface area and micropore volume of the samples were measured using N_2 adsorption-desorption (AUTOSORB 1C, Quantachrome Corp., USA) at −196 °C. Prior to adsorption, the samples were evacuated until a pressure of 66.6 Pa at room temperature was reached, then heated to 50 °C and evacuated until a pressure of 1.3 Pa was reached. This condition was maintained overnight. The surface area, total pore volume and micropore volume were determined by multipoint BET, DFT (Density Functional Theory) and DR (Dubinin-Radushkevich), respectively [34]. The pH at the point zero charge (pH_{pzc}) of pine sawdust treated with sulfuric acid was fixed, as described by Ferro-Garcia et al. [18]. To specify the pH_{pzc}, 50 ml NaCl solution (0.01 M) and 1.0 g of APSD were put in the Erlenmeyer flask. The pH within every Erlenmeyer flask was set between 1-12 as a result of adding HCl or NaOH. Afterward, the Erlenmeyer flasks were agitated at 125 rpm for 24 h, and the final pH was measured. The difference between the initial and final pH was plotted versus the initial pH. The intersection point of this curve provided the pH_{pzc}.

4. Adsorption Experiments

Adsorption experiments with raw and pretreated pine sawdust were performed with a working volume of 100 ml of the desired dye concentration by a thermoshake incubator shaker (Gerhardt, Germany) at a constant speed (125 rpm) and constant temperature (25 °C). After equilibration, to take the adsorbent particles from the medium, the solution was centrifuged for 10 min at 3,000 rpm, and the final concentration of MR GRL was determined by utilizing a UV-Visible spectrophotometer (Spectroquant Pharo 300, Merck) at the wavelength of λ_{max}=531 nm. The MR GRL concentration was calculated by the comparison of absorbance with the dye calibration curve that had been acquired before. Blank runs were carried out with only the adsorbent in 100 ml of double-distilled water in a simultaneous manner under identical conditions to explain any color leached by the adsorbents and adsorbed by glass containers.

The experiments were performed in duplicate, and the mean values were utilized for calculations. The maximum deviation was found as ±2%. The experimental conditions of the adsorption study carried out under different experimental conditions are shown in Table 1.

During the analysis, the values of percentage removal and the amount of the dye adsorbed were calculated using the following equations:

$$\text{Dye removal}\ (\%) = \frac{C_i - C_e}{C_i}\ 100 \tag{1}$$

$$q_e = \frac{(C_i - C_e)V}{m} \tag{2}$$

where q_e denotes the adsorption capacity (mg/g), C_i and C_e denote the initial and equilibrium dye concentration, respectively (mg/L), and m denotes the adsorbent dose (g), and V denotes the volume of the dye solution (L).

5. Adsorption Kinetics and Isotherms

Adsorption kinetic studies were carried out in 250 ml flasks which contained 100 ml of MR GRL dye (500 mg/L) solution with 4-8-

Table 1. Experimental conditions of adsorption study

Process parameter varied	Initial dye conc. (mg/L)	Dose (g/L)	Contact time	Initial pH	Temperature (K)
Pretreatment (H_2SO_4, NaOH)	100-150-200-250-500	8	24 hours	Solution pH	298
Contact time (kinetic study)	500	4-8-10	0-300 min	Solution pH	298
Initial pH	500	8	180 min	1-8	298
Initial dye concentration (isotherm study)	250-500-750-1000	8	180 min	Solution pH	298
Temperature (thermodynamic study)	250-500-750-1000	8	180 min	Solution pH	298, 308, 318
Ionic strength	250	8	180 min	Solution pH	298

*Solution pH: 5.7-6.0

10 g/L of APSD. A shaker was used to stir the volumetric flasks at 125 rpm at 298 K. The specimens were obtained at varied time intervals and centrifuged, and the supernatant dye concentration was analyzed. The data obtained were studied using the pseudo-second-order, Ritchie's-second-order, Elovich, and Weber-Morris kinetic models.

For the equilibrium adsorption experiments, APSD adsorbent (8 g/L) was mixed with solutions of various initial MR GRL concentrations (250-1,000 mg/L) at a natural solution pH, at 298 K for 180 min to ensure the adsorption equilibrium. Afterward, samples were collected, centrifuged, and then the obtained supernatant was analyzed in terms of MR GRL concentration. The equilibrium data of MR GRL dye adsorption on APSD was analyzed by employing the Langmuir, Freundlich, Temkin, R-P, and D-R isotherm models.

Non-linear regression was used to define kinetic and isotherm model data. The suitability of the studied models was evaluated using R^2, SSE, and RMSD. The correlation coefficient (R^2), the adjusted determination coefficient (R^2_{adj}, Eq. (3)), the sum of the squares of the errors (SSE, Eq. (4)), and root-mean-square deviation (RMSD, Eq. (5)) were examined using Microsoft Excel for all sets of experimental data. R^2_{adj} represents a modified R^2, adjusted for several terms in the model. Differently from R^2, when terms are added to the model, R^2_{adj} may take a smaller value [12].

$$R^2_{adj}=1-(1-R^2)\left(\frac{n-1}{n-p}\right) \quad (3)$$

where p refers to the number of the fitted model's parameters. R^2 shows how much of the variability observed in the data was explained by the model, whereas R^2_{adj} modifies R^2 by considering the number of the model covariates or predictors. R^2_{adj} close to the values of R^2 ensures that quadratic models are adjusted to the experimental data in a satisfactory way. Thus, the removal efficiency was explained by the regression models well [37].

$$SSE=\Sigma_{n=1}^{p}(q_e^{cal}-q_e^{exp})\frac{2}{n} \quad (4)$$

$$RMSD=\frac{\sqrt{\Sigma_{i=1}^{n}(q_{exp}-q_{cal})^2}}{n-1} \quad (5)$$

where n denotes the number of experimental data, while q_{exp} (mg/g) and q_{cal} (mg/g) denote the experimental and computed adsorption capacity, respectively [38].

Furthermore, the suitability of the kinetic model for the purpose of describing adsorption was further confirmed by the normalized standard deviation, Δq (%), presented in the equation [38]:

$$\Delta q=100\sqrt{\frac{\Sigma[(q_{exp}-q_{cal})/q_{exp}]^2}{n-1}} \quad (6)$$

6. Impact of Ionic Strength

Adsorption is sensitive to changes in ionic strength. The wastewater has commonly higher salt concentration, which makes it necessary to study the effects of ionic strength on the adsorption of dye. Two probable impacts of salts during the wastewater treatment are as follows: (i) The equilibrium dye removal generally decreases, (ii) Contrary to expectations, dye removal increases as the dye dissolution may be increased by the existence of foreign salts [39]. Hence, the current research investigated the impact of ionic strength on the adsorption efficiency of the adsorbent. The impact of ionic strength on the MR GRL dye adsorption was tested by adding NaCl, SDS, and CTAB at 0.05-0.25 mol/L concentrations to the solution.

RESULTS

1. Characterization

1-1. pH_{pzc}

In physical chemistry, the pH at the point zero charge (pH_{pzc}) represents a concept used for an understanding of the adsorption mechanism in a better way. The pH_{pzc} is a significant characteristic since it indicates the adsorbent's acidity or basicity and the net surface charge of the adsorbent in the solution. Therefore, the pH of the point zero charge (pH_{pzc}) was measured. The surface is negatively charged in case of pH higher than pH_{pzc}, and the adsorption of cations is preferred. It is positively charged in case of pH lower than pH_{pzc}, and anions are adsorbed [40]. The pH_{pzc} was found to be 4.50 (Fig. 2). According to the results, the adsorption of cations will be more favorable since $pH>pH_{pzc}$.

1-2. SEM Images and EDX Spectra

Fig. 3 demonstrates the SEM analysis results for raw and acid-pretreated pine sawdust at 500x magnification. The SEM images show that the surface of PSD (Fig. 3(a)) was abundant in regular pores of uniform size. The generation of a new surface area by acidification was observed. The results effectually displayed that bigger pores were formed through the pretreatment procedure. The porosity developed through the pretreatment process mainly depends on two factors: the activation condition and the nature of the material [41]. APSD has micro and macroporous spaces and large cavities with a high possibility for dye adsorption (Fig. 3(b)). The size and shapes of the pores are irregular. The above-mentioned characteristics demonstrate that APSD has strong adsorption features to remove MR GRL from the aqueous solution. It is possible to show Fig. 3(c) as evidence for these explanations because MR GRL dye molecules cover the APSD surface.

Energy-dispersive X-ray analysis (EDX), represents a common tool for accompanying SEM, as well as TEM. The composition of the acid-pretreated pine sawdust was studied using EDX. The EDX spectra (Fig. 4(a)) show that APSD is primarily composed of C and O, and S and Br trace amounts. Following adsorption, Zn and Cl peaks in the spectrum can be observed due to $ZnCl_3^-$ in the chemi-

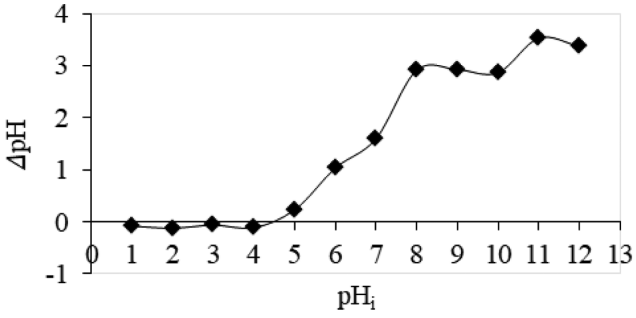

Fig. 2. pH_{pzc} of APSD.

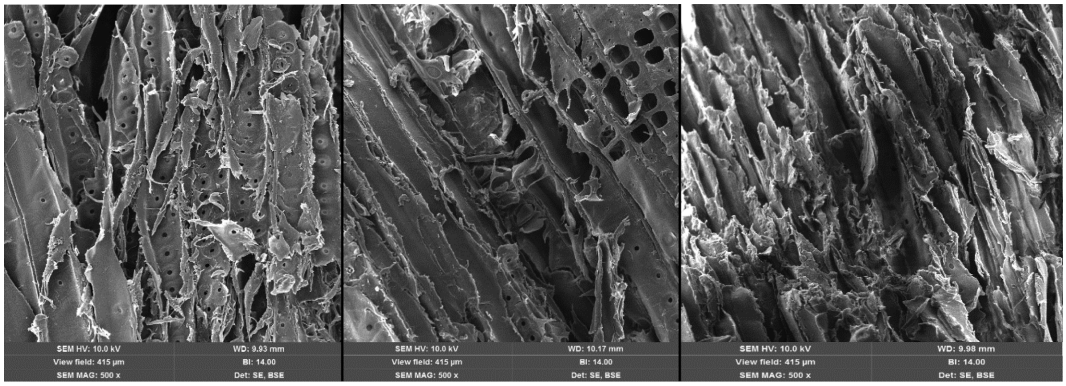

(a) (b) (c)

Fig. 3. SEM images of adsorbents (a) PSD (b) APSD before MR GRL adsorption (c) APSD after MR GRL adsorption.

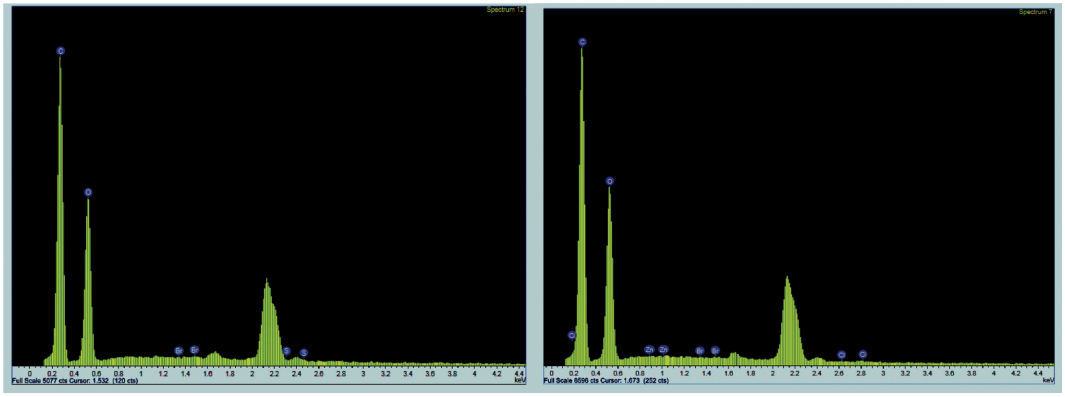

(a) (b)

Fig. 4. EDX spectra of APSD (a) before MR GRL adsorption (b) after MR GRL adsorption.

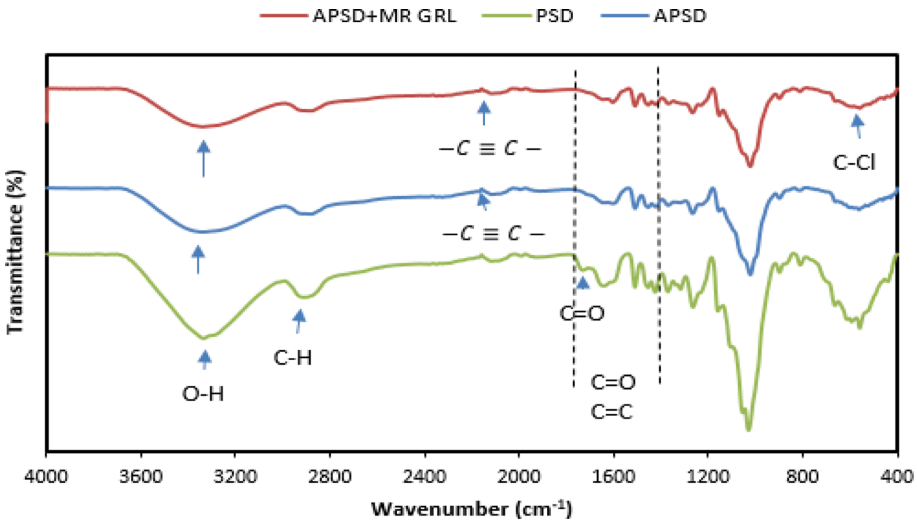

Fig. 5. FTIR spectra of PSD, APSD and APSD+MR GRL.

cal formula of MR GRL (Fig. 4(b)), while S peaks are decreased. Fig. 4(b) indicates the successful MR GRL adsorption onto APSD.

1-3. Fourier Transform Infrared Spectrum

The FTIR analysis was conducted to determine the potential interactions between the functional groups of adsorbents (PSD and APSD) and MR GRL dye cations. Fig. 5 demonstrates the FTIR spectra of PSD and APSD prior to the dye treatment and the FTIR spectra of APSD following the dye treatment. The spectra show several absorption peaks, representing the adsorbent's complex character. The alterations determined in the spectrum indicate the

potential engagement of functional groups on the adsorbent's surface in adsorption.

The strong and broad peaks at 3,000-3,500 cm^{-1} are characterized as the O-H stretching bond structure because of the O-H groups that are mainly found in cellulose. The peak at a wavelength of 2,913 cm^{-1} is characterized as the C-H bending bond from the functional group of alkanes (lignin, cellulose, and hemicellulose). Finally, the band at 1,730 cm^{-1} was assigned to carbonyl groups (C=O). This band exists in different hemicellulose types [28]. The low signal intensity possibly resulted from the low concentration of the substance in question in PSD (Fig. 5(a)).

The peak at 2100-2260 cm^{-1} corresponded to the -C≡C- stretching vibrations, indicating the existence of the alkyne group. The presence of aromatic (=C-H) compounds was demonstrated by the peak at 1,600-2,000 cm^{-1}. C=C and C=O stretching absorptions were found at 1,400-1,750 cm^{-1} for the aromatic ring. The attenuated band at a wavelength of 1,265 cm^{-1} corresponded to the C-O group, which represents a feature of esters, alcohols, and carboxylic acids, all of which are found in the molecular structures of the main components of APSD. Furthermore, when other absorption peaks are evaluated, it is evident that the existence of carbonyl groups, hydroxyl groups, aromatic compounds, and ethers represents a confirmation of the lignocellulosic structure of pine sawdust [42].

The peak at 1,080-1,360 cm^{-1} corresponds to the C-N stretching vibration, which demonstrates the existence of amines. The peak at 675-1,000 cm^{-1} corresponds to the =C-H stretching vibrations, which shows the presence of alkenes. The adsorption band at 730-550 cm^{-1} corresponds to the C-Cl bending stretch. In this band, -Cl is attached to the adsorbent from the chemical structure of MR GRL. According to Fig. 5(b), (c), FTIR spectra did not display very significant changes, but only a few peaks were shifted or appeared due to MR GRL adsorption onto APSD. The spectrum of APSD+MR GRL exhibits one strong band at a wavelength of 1,422 cm^{-1}, which is a characteristic of MR GRL. It can be deduced that MR GRL molecules were successfully adsorbed onto APSD. Furthermore, small changes in peaks are evidence that MR GRL dye attaches onto APSD by the physical adsorption process.

1-4. Surface Area and Pore Characteristics

Nitrogen adsorption-desorption isotherm experiments were performed to determine Brunauer-Emmett-Teller (BET) specific surface areas (S_{BET}), pore volumes and pore sizes of adsorbent before and after H_2SO_4 treatment (Table 2 and Fig. 6). The adsorption-desorption isotherms of samples are of type III (BET classification) according to the IUPAC classification [43], suggesting that samples contain micro- and mesoporous that allow the formation of multiple adsorbent layers with increasing P/P^o. With the acid activation of PSD, some of the existing bonds might be broken and new bonds may be formed. It might be due to the formation of micropores. The surface area, pore size and micropore volume of samples treated with H_2SO_4 significantly increased due to the decomposition of lignin, hemicellulose, and cellulose with the chemical activation. As seen in Table 2, with the chemical activation of the PSD increased the total surface area from 3.97 m^2/g to 19.11 m^2/g.

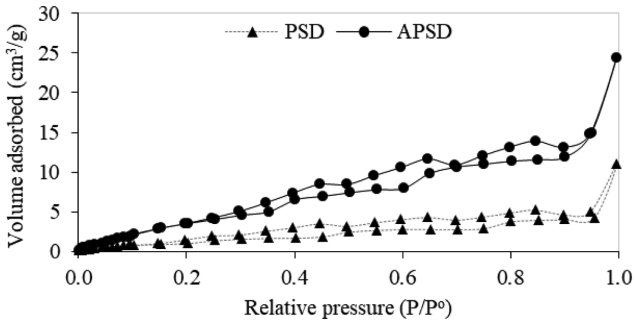

Fig. 6. The nitrogen adsorption-desorption isotherm of PSD and APSD.

2. Impact of Adsorbent Pretreatment

Chemical activating agents, such as NaOH, $CaCl_2$, HCl, KOH, H_3PO_4, and H_2SO_4, are used to modify an adsorbent to increase its efficiency for adsorption [44]. In this study, H_2SO_4 and NaOH were selected as chemical activation agents. Experiments were carried out using PSD, BPSD, and APSD at 8 g/L a constant adsorbent dose, pH (5.7-6.0), and temperature (298 K) for 24 h at varying Maxilon Red GRL concentrations (100-500 mg/L). The impact of the adsorbent pretreatment with NaOH and H_2SO_4 on the uptake and yield of adsorption was studied (Fig. 7). It is clearly shown in Fig. 7 that increasing the concentration from 250 mg/L resulted in a significant decrease for PSD and BPSD in the adsorption uptake. However, even at a higher concentration, the adsorption efficiency for APSD increased. APSD had higher adsorption efficiency than that of PSD and BPSD for all the dye concentrations studied.

Since pretreatment with inorganic acids, such as HCl, H_2SO_4, and

Table 2. The surface area and pore characteristics of natural (PSD) and acid activated pine sawdust (APSD)

	PSD	APSD
S_{BET} [a] (m^2/g)	3.97	19.11
V_{Total} [b] (cm^3/g)	0.007	0.02
V_{micro} [c] (cm^3/g)	0.0016	0.0065
D_p [d] (Å)	33.17	24.21

[a]Multipoint BET method.
[b]Volume adsorbed at P/P^o=0.99.
[c]Micropore volume calculated by DR method.
[d]Average pore diameter determined by DFT.

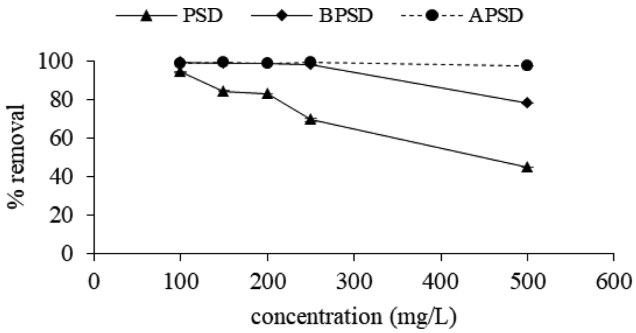

Fig. 7. Effect of adsorbent pretreatment on MR GRL adsorption.

HNO_3, increases the porosity and surface area of the adsorbent material, the yield of the adsorbent increases further [45]. According to Fig. 7, the treatment of pine sawdust with acids significantly improves the adsorption characteristics of the materials with regard to dye cleaning from the aquatic medium. The removal of MR GRL dye was 99.35%, 99%, and 69.44% by APSD, BPSD, and PSD, respectively, at a dye concentration of 250 mg/L. The adsorption efficiency of BPSD and APSD was almost identical when the initial dye concentration in wastewater reached 250 mg/L. However, the adsorption efficiency at higher dye concentrations was APSD>BPSD> PSD. At a concentration of 500 mg/L, the efficiency of APSD was 2.5 times higher compared to PSD. It was decided that it would be appropriate to continue conducting research with pine sawdust pretreated with H_2SO_4 (APSD) in future studies.

3. The Impact of the Contact Time and Initial Adsorbent Concentration (Kinetic Study)

Adsorption kinetic studies are essential to treat aqueous effluents since they give useful data on the adsorption mechanism. The rate of adsorption can be fitted, the adsorption mechanism can be "meaned", and a reasonable adsorption kinetic model can be installed [46]. For kinetic studies, 0.4, 0.8, and 1.0 g/100 ml of APSD were contacted with 100 ml of 500 mg/L MR GRL dye solution. The MR GRL adsorption on APSD was analyzed depending on contact time for the purpose of determining the required adsorption equilibrium time. An increase from 83.1% to 95.4% occurred in the adsorption efficiency with an increase in the APSD dose from 0.4 to 1.0 g/100 ml at equilibrium time (Fig. 8). The increased adsorption with an increase in the adsorbent dosage may be explained by the increasing adsorbent surface area and availability of more adsorption sites. Sorption was very quick at the beginning for all three adsorbent doses. Approximately 94% of the dye was removed after 60 min of contact with the sorbent and equilibrium was slowly achieved within 180 min. Prolonging the contact time more did not increase the adsorption capacity of the adsorbent for MR GRL. The equilibrium time was set to 180 min for subsequent studies. The high rate at the beginning may be related to an excess of available areas on the adsorbent surface. However, the adsorption rate decreased afterward, possibly due to the gradual filling of these free binding sites [18]. The highest removal of MR GRL dye was determined at the amount of the adsorbent equal to 8 g/L. An additional increase higher than the adsorbent dose of 8 g/L did not increase MR GRL removal, and the removal efficiency remained constant. The above-mentioned situation demonstrates that the optimum adsorbent amount needed for MR GRL dye removal is 8 g/L.

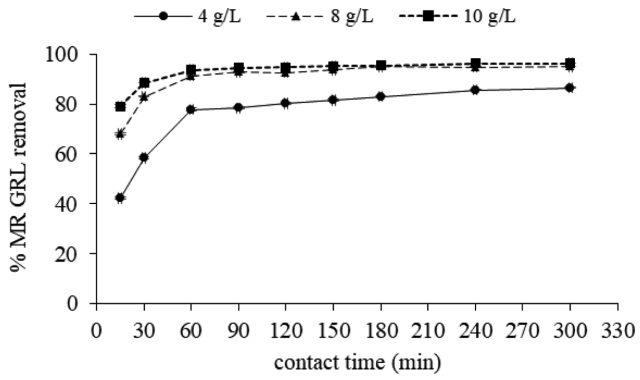

Fig. 8. Effect of adsorbent dosage.

3-1. Kinetics of Adsorption

For the purpose of studying the controlling mechanism of sorption, including diffusion control, chemical reaction, and mass transfer, a few kinetic models were utilized for the purpose of testing experimental data. The kinetic parameters that can help in predicting the adsorption rate provide significant data for designing and modeling adsorption [47]. Therefore, Ritchie's second-order, pseudo-second-order, Weber-Morris, and Elovich kinetic models were utilized for the analysis of the experimental data in order to reveal the adsorption mechanism, e.g., diffusion and adsorption. Kinetic constants were found for the equations in Table 3 utilized for the description of the adsorption kinetics of MR GRL on APSD. The kinetic constants, correlation coefficients, SSE, and RMSD values were determined by plotting q_e versus t, and the values are shown in Table 3.

As the correlation coefficients of the pseudo-first-order reaction for all three samples were found to be much lower than 0.68, the results were not given in Table 3. The above-mentioned situation demonstrates that MR GRL adsorption onto APSD is not ideal for the pseudo-first-order reaction. It is possible to describe adsorption by the pseudo-second-order and Ritchie's-second-order kinetic models. Furthermore, the calculated values of adsorption capacities (q_e, cal) obtained from plots are close to the experimental values (q_e, exp) (Table 3), indicating that the reaction of adsorption is compatible with these two kinetic models. However, the best linearity in comparison with other kinetic models was obtained for the pseudo-second-order kinetic model as seen in Table 3, with the correlation coefficients greater than $R^2 \geq 0.9999$ and lower values of the SSE function for all APSD doses, which proves a great fit of the model in question to experimental points.

However, the pseudo-second-order kinetic model is not capable of describing the diffusion mechanism alone. The transfer of the dissolved matter in an adsorption system can be characterized by intra-particle diffusion or by both models [48]. Therefore, to explain the mechanism of diffusion, the intra-particle diffusion model (Weber-Morris) was implemented in the present work data. Accordingly, if a straight line that passes through the origin is obtained by the Weber-Morris plot of q_t versus $t^{1/2}$, intra-particle diffusion alone controls adsorption. However, in the case of the data showing multi-linear plots, two or more steps affect adsorption [49]. The plots obtained from Weber-Morris did not yield a straight line that passed through the origin for all the adsorbent dosages. It was possible to separate them into two or three linear regions. This situation shows the presence of multiple stages to the process of adsorption. The R^2 values lower than 0.9 (Table 3) demonstrate that intra-particle diffusion cannot describe the adsorption of MR GRL on APSD, and due to the mentioned lines not passing through the origin, it is possible to reach a conclusion that Weber-Morris model alone does not represent the rate-controlling step.

4. Impact of Initial pH

The pH of a solution is among the most significant parameters that control adsorption, and thus, it should be found. The characteristic and degree of ionization of the adsorbate and the surface

Table 3. Parameters of kinetic models for the adsorption of MR GRL on APSD at different initial adsorbent doses

Kinetics	Adsorbent dose		
	4 g/L	8 g/L	10 g/L
Ritchie's-second-order	$\frac{1}{q_t}=\frac{1}{kq_e t}+\frac{1}{q_e}$		[50]
Fitted model	$1/q_t=1.7283\frac{1}{t}+0.099$	$1/q_t=1.2095\frac{1}{t}+0.1852$	$1/q_t=0.799\frac{1}{t}+0.2327$
R^2	0.999	0.996	0.992
Constant, k min^{-1}	0.057	0.153	0.291
q_e, ($q_{e,cal}$)	10.100	5.400	4.297
q_e, ($q_{e,exp}$)	9.150	5.236	4.202
Δq*	0.672	0.116	0.067
SSE	0.159	0.297	0.176
RMSD	4.986	5.548	5.238
R^2_{adj}	0.998	0.996	0.991
Pseudo-second-order	$t/q_t=(1/k_2q_e^2)+t/q_e$		[51]
Fitted model	$t/q_t=1.7117+0.0992t$	$t/q_t=1.0291+0.1871t$	$t/q_t=0.7912+0.2328t$
R^2	0.999	0.999	1.000
Constant, k_2, g/(mg min)	5.75×10^{-3}	0.034	0.069
q_e, ($q_{e,cal}$), mg/g	10.080	5.345	4.295
q_e, ($q_{e,exp}$)	9.150	5.236	4.202
Δq*	0.657	0.077	0.066
SSE	0.109	0.257	0.067
RMSD	0.041	0.063	0.032
R^2_{adj}	0.999	0.999	1.000
Weber-Morris	$q_t=k_d\,t^{1/2}+C$		[52]
Fitted model	$q_t=0.33\,t^{1/2}+4.631$	$q_t=0.0939\,t^{1/2}+3.3095$	$q_t=0.0464\,t^{1/2}+3.5764$
R^2	0.821	0.709	0.709
Constant, k_d, mg/g $min^{-0.5}$	0.330	0.094	0.046
SSE	3.804	0.581	0.142
RMSD	0.244	0.095	0.047
R^2_{adj}	0.796	0.668	0.668
Elovich	$q_t=\beta\ln(\alpha)+\beta\ln t$		[53]
Fitted model	$q_t=0.8365\ln(\alpha)+1.6105\ln t$	$q_t=2.7549\ln(\alpha)+0.4734\ln t$	$q_t=3.0129\ln(\alpha)+0.233\ln t$
R^2	0.949	0.875	0.869
Constant α, mg/g min	$\alpha=1.681$	$\alpha=336.767$	$\alpha=412875.46$
β	$\beta=1.611$	$\beta=0.473$	$\beta=0.233$
SSE	1.071	0.249	0.064
RMSD	0.129	0.062	0.032
R^2_{adj}	0.943	0.858	0.850

*Δq=The standard deviation between the experimental and calculated adsorption capacities.

load of the adsorbent are affected by the pH of the solution [54]. Fig. 9 demonstrates the impact of pH on the MR GRL percentage adsorbed by APSD. When an increase from 1 to 5 occurred in the initial pH, the capacity of sorption increased from 39.28 to 55.05 mg/g, and the performance of the dye removal increased significantly from 70.05% to 98.19%, respectively. At higher pH values of 5-8, the dye adsorption remained almost constant, and the maximum dye removal within this pH range was 98.31% (Fig. 9). This result is due to the effect of ionic interaction on adsorption. Because the adsorbent surface charge is positive at a lower pH value, the competitive impacts of the surrounding H^+ ions and electrostatic repulsion between the dye cation and the positively charged active adsorption sites on the adsorbent surface cause the decreased dye removal. Otherwise, as pH increases, further adsorption of the cationic dye is provided as the adsorbent surface will have a negative charge due to the electrostatic attraction forces [18].

It is possible to describe the impact of pH on adsorption by APSD based on the pH_{pzc} with the neutral adsorbent. The pH_{pzc} of APSD was 4.50. The adsorbent's surface charge is positive in case of the pH of the medium lower than the pH_{pzc} value, whereas it is

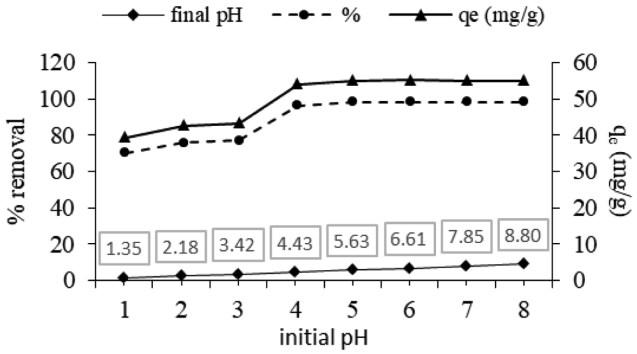

Fig. 9. Effect of pH on adsorption of MR GRL dye by APSD.

negative at a pH value above the pH_{pzc} [20,22,23]. Therefore, for a pH higher than 4.50, an increase occurred in the negative charge density of APSD, which facilitated the adsorption of the cationic dye. Therefore, the natural pH (5.7-6.0) was chosen to carry out further investigations.

5. Impact of the Initial Dye Concentration

The removal of pollutants at high concentrations takes place among the success parameters utilized for the assessment of the effectiveness of the treatment. Thus, at the phase in question, MR GRL concentrations that changed between 250 and 1,000 mg/L were investigated at three various temperatures, 298, 308, and 318 K, for the constant APSD dose of 8.0 g/L and the natural pH of 5.7-6.0. The efficiency values acquired as a function of equilibrium time are demonstrated in Fig. 10.

As observed in Fig. 10(a), the removal percentage of the dye decreased from 98.94% to 92.86% with the increasing initial dye concentration from 250 to 1,000 mg/L at 298 K, respectively. The decreasing initial dye concentration causes an increased total number of active binding sites. Hence, a higher removal percentage of MR GRL was reached at the initial concentration of 250 mg/L. However, when the temperature was 308 and 318 K, the removal efficiency was constant at values above 99.7% at all the studied dye concentrations, which demonstrated that the increase in the temperature did not cause a significant increase in the removal efficiency. As seen in Fig. 10(a), for the equilibrium time of 180 min, the efficiency values of 92.85, 99.36, and 99.59% were acquired at the temperatures of 298, 308, and 318 K, respectively, at the dye concentration of 1,000 mg/L. The adsorption capacity of APSD did not change significantly with the increasing temperature.

Although a decrease in the removal efficiency (%) occurred with the increased initial dye concentration at 298 K, the equilibrium adsorption capacity (q_e) increased from 30.59 to 116.35 mg/g with the increased initial dye concentration (Fig. 10(b)). The increased dye concentration leads to the speeding of the diffusion of dyes from the solution onto adsorbents because of the increased driving force of the concentration gradient [21]. Thus, an increase took place in the actual amount of the dye adsorbed (q_e) with an increase in the concentration of the initial dye solution but did not change with an increase in the temperature. This reveals that a higher temperature is not required for the MR GRL removal by adsorption on APSD, and the adsorption of MR GRL on APSD was exothermic in nature.

5-1. Adsorption Isotherms

The adsorption isotherm represents the equilibrium relation between the quantity of the adsorbate per unit of the adsorbent (q_e) and its equilibrium solution concentration (C_e) at a constant temperature [55]. It is crucial to develop a suitable isotherm model for adsorption for designing and optimizing adsorption. Isotherms are frequently utilized for the purpose of describing the equilibrium behavior of the adsorption process. Equilibrium sorption is generally defined by the isotherm equation characterized by some parameters expressing the interest of the adsorbent in the substance to be adsorbed and the surface properties of the sorbent [56,57].

Experiments to estimate the adsorption isotherms of MR GRL onto APSD were conducted at three temperatures with different concentrations of MR GRL. The experimental data points and the theoretical isotherm plots are compared in Fig. 11. As seen, the D-R isotherm deviates from the experimental data at all three temperature values. Since the R-P isotherm data significantly deviates from the experimental data, they are not shown in the graph.

For the purpose of providing more data on the MR GRL adsorption onto APSD, the results of the equilibrium experiments were assessed by the Langmuir, Freundlich, Dubinin-Radushkevich, Redlich-Peterson, and Temkin models. Table 4 presents all the isotherm parameters and the results of nonlinear regression for different dye concentrations and temperatures. The best isotherm model is based on higher correlation coefficient values (R^2) with low error values. Based on the R^2 comparison, we reached a con-

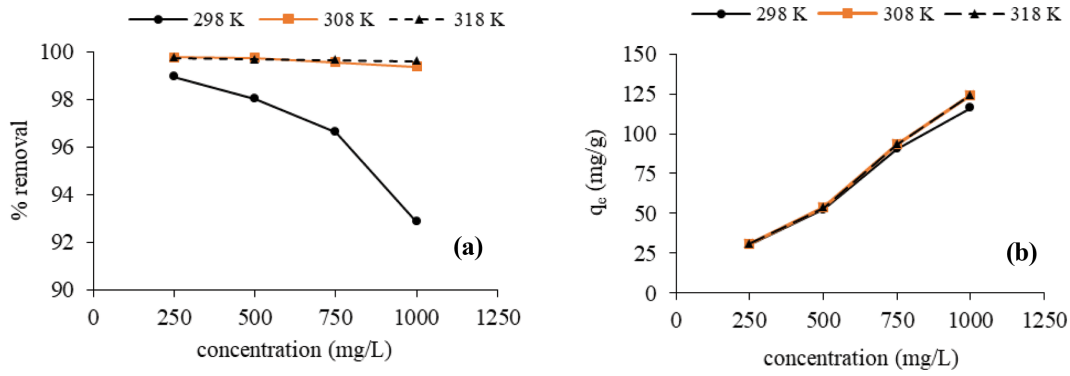

Fig. 10. Effect of dye concentration and temperature on the adsorption of MR GRL onto APSD (a) removal (%) (b) q_e (mg/g).

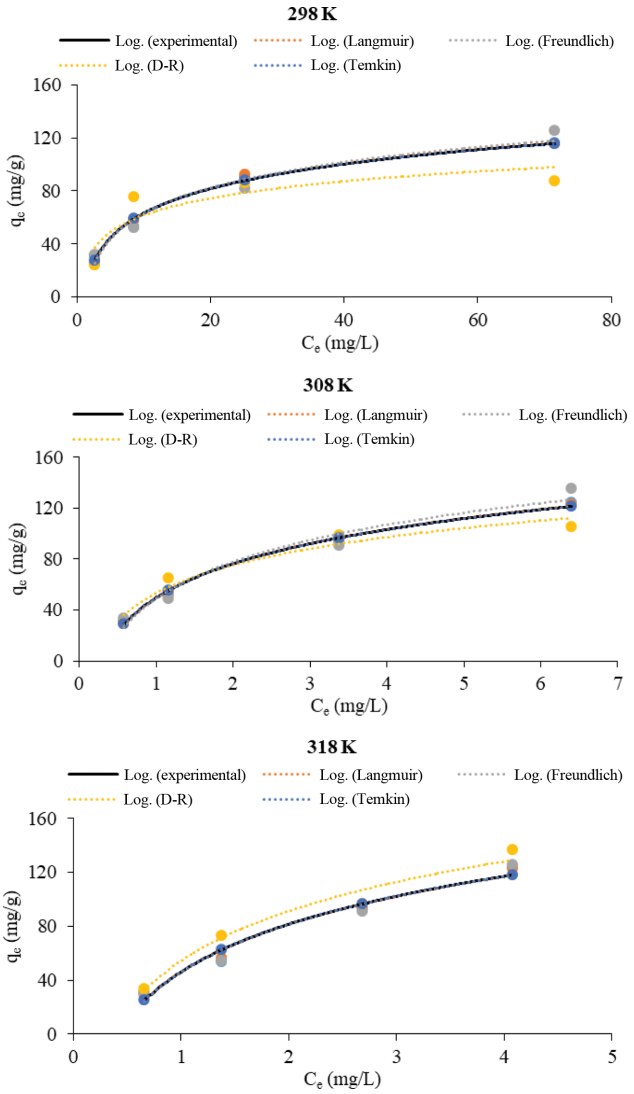

Fig. 11. Adsorption isotherms for the adsorption of MR GRL onto APSD at different temperatures.

clusion that the D-R, R-P, and Temkin isotherms had a smaller R^2 value in comparison with the remaining models. The adsorption isotherm fits the Langmuir and Freundlich models well. Nevertheless, it is more suitable to compare the goodness of fit to isotherms using the error values. Therefore, the SSE and RMSD values were contrasted for all the isotherms. The best-fit model is required to have a minimum SSE value. The Langmuir isotherm model was revealed to provide satisfactory results in the description of the adsorption equilibrium since the minimum SSE and RMSD values and R^2 were above 0.99.

Monolayer adsorption on the homogeneous surface that contains a limited number of adsorption sites without transmigration of the adsorbate on the surface is assumed by the Langmuir model [58]. Furthermore, equal energies of adsorption onto the surface without transmigration of the adsorbate on the plane of the surface or in the inner surface of the adsorbent are assumed in the Langmuir model. If the adsorbent surface contains a limited number of similar sites, the Langmuir isotherm is appropriate for monolayer adsorption onto it [59].

The favorability of MR GRL dye adsorption onto APSD was further evaluated by the dimensionless constant separation factor, R_L, derived from the Langmuir model. In case of $0<R_L<1$, there is favorable adsorption; in case of $R_L>1$, there is unfavorable adsorption; if $R_L=1$, there is linear adsorption; and adsorption is irreversible if $R_L=0$ [50,60]. In Table 4, the R_L value (the separation factor for C_i=250 mg/L) is $0<R_L<1$ (Note: $0<R_L<1$ also for other concentrations), indicating that the process of adsorption was favorable and adsorption was good.

According to the results of the present study, the maximum sorption capacity (Q_{max}) was 312.5 mg/g, and Langmuir isotherm constant (k_L) was 0.158 L/mg at 318 K. The R^2 value of 0.9922 proved that there was a good fit of the sorption data to the Langmuir isotherm model (Table 4).

It is possible to apply the Freundlich model to multilayer adsorption, with adsorption heat and affinities distributed nonuniformly over the heterogeneous surface [61]. The above-mentioned model indicates that there will be an increase in the adsorbate concentration on the adsorbent along with the increasing adsorbate concentration in the solution, with the graph not reaching saturation [62]. Table 4 also presents the value of n found from the Freundlich equation. The n value demonstrates the nonlinearity degree between the adsorbate concentration and adsorption. The adsorption process is linear for n=1; if n<1, it specifies the chemisorption process; and n>1 implies a physical process. The case of n>1 is the most frequently encountered and may be caused by a distribution of surface sites or any factor that leads to decreased interaction between the adsorbent and adsorbate with an increase in surface density [63]. In the current research, the value of n was determined as n>1 at all the investigated temperatures, suggesting the favorable adsorption and the physical adsorption of MR GRL onto APSD.

The D-R isotherm model represents an empirical model generally used for describing the sorption of vapors onto microporous solids with the aim of expressing the adsorption mechanism with a Gaussian energy distribution on a heterogeneous surface. This model assumes that a pore-filling mechanism is followed by adsorption, and it has been employed for the purpose of distinguishing the chemical and physical adsorption using isotherm parameters concerning sorption energy [64]. The linear regression values from Table 4 demonstrate that the adsorption process was not fitted to the D-R isotherm model due to unsatisfactory R^2 values. The E value for the D-R isotherm is very beneficial for predicting the type of adsorption. If E is lower than 8 kJ/mol, adsorption is a physical process (physisorption) with van der Waals interactions. If 8<E< 16 kJ/mol, adsorption is a chemical process with higher sorption enthalpy, more likely caused by the ion-exchange mechanism. In this research, E was found to be 0.5, 1.581, and 1.581, respectively, so the sorption mechanism was physical.

The Temkin isotherm model estimates a decrease in the adsorption heat in a linear way with the increasing surface coverage. The mentioned isotherm includes a factor, definitely considering interactions between the adsorbate and adsorbent. The model is valid only for a specific adsorbate concentration range [65]. The Temkin model represents an appropriate model for the chemical adsorp-

Table 4. Equilibrium modeling for the adsorption of MR GRL by the APSD

Isotherm models	Temperature, K		
	298	308	318
Langmuir		$1/q_e=1/C_e\ k_L\ Q_o+1/Q_o$	[59]
Fitted model	$C_e/q_e=0.0836+0.0075C_e$	$C_e/q_e=0.0157+0.0057C_e$	$C_e/q_e=0.0202+0.0032C_e$
Q_{max} [mg/g]	133.33	175.44	312.5
k_L [L/mg]	0.089	0.363	0.158
$R_L=1/(1+k_LC_o)$	0.043	0.011	0.025
R^2	0.996	0.996	0.992
SSE	0.001	0.000	0.000
RMSD	0.008	0.001	0.001
R^2_{adj}	0.994	0.994	0.989
Freundlich		$\log(q_e)=\log(K_F)+1/n\log(C_e)$	[67]
Fitted model	$\ln q_e=3.0661+0.4135\ \ln C_e$	$\ln q_e=3.8077+0.5726\ \ln C_e$	$\ln q_e=3.7501+0.7703\ \ln C_e$
K_F [mg/g]	21.458	42.525	45.047
n	2.42	1.30	1.75
R^2	0.983	0.999	0.985
SSE	0.018	0.001	0.017
RMSD	0.045	0.011	0.043
R^2_{adj}	0.974	0.999	0.978
Dubinin-Radushkevich		$\ln q_e=\ln q_m-K_{DR}\varepsilon^2$	[62]
Fitted model	$\ln q_e=4.4714-2E\text{-}06\varepsilon^2$	$\ln q_e=4.6823-2E\text{-}07\varepsilon^2$	$\ln q_e=4.7085-2E\text{-}07\varepsilon^2$
$K_{DR}\times10^7$ [mol^2/kJ^2]	20	2	2
$E=1/\sqrt{2K_{DR}}$ [kJ/mol]	0.500	1.581	1.581
q_m [mg/g]	87.48	108.02	110.89
R^2	0.782	0.939	0.904
SSE	0.268	0.071	0.139
RMSD	0.173	0.089	0.124
R^2_{adj}	0.673	0.908	0.856
Temkin		$q_e=B\ln A+B\ln C_e$	[68]
Fitted model	$q_e=26.712\ \ln C_e+1.7184$	$q_e=38.682\ \ln C_e+49.535$	$q_e=51.125\ \ln C_e+46.09$
A [L/mg]	1.066	3.599	2.463
B [J/mol]	26.712	38.682	51.125
R^2	0.987	0.995	0.966
SSE	55.985	27.237	173.090
RMSD	2.494	1.740	4.385
R^2_{adj}	0.981	0.992	0.949
Redlich-Peterson		$\log\left[\left(\frac{K_{RP}C_e}{q_e}\right)-1\right]=\beta\log C_e+\log(\alpha_{RP})$	[62]
Fitted model	$\log\left[\left(\frac{K_RC_e}{q_e}\right)-1\right]=1.6575\log C_e-2.0425$	$\log\left[\left(\frac{K_RC_e}{q_e}\right)-1\right]=1.0262\log C_e-0.4568$	$\log\left[\left(\frac{K_RC_e}{q_e}\right)-1\right]=1.3411\log C_e-0.9473$
$K_R=q_{max}\ k_L$ [L/g]	11.960	63.690	49.380
β	1.658	1.026	1.341
α_{RP} [L/mg]	110.280	2.860	8.860
R^2	0.889	0.996	0.917
SSE	0.391	0.003	0.059
RMSD	0.208	0.018	0.081
R^2_{adj}	0.668	0.988	0.750

tion on the basis of powerful electrostatic interaction occurring between negative and positive charges [66]. The model was consistent with the experimental data (R^2>0.9). However, higher values of SSE and RMSD prove that the Temkin model cannot be

Table 5. Comparison of maximum adsorption capacity of various adsorbent for MR GRL

Adsorbent	Maximum adsorption capacity, Q_{max}, (mg/g)	Reference
Niğde (Bor) grape molasses soil	7.68	[69]
Waste activated sludge (WS)	58.82	[70]
Oak acorn starch, sorghum starch, potato starch	12.67, 16.75, 28.57	[71]
Walnut shell	36.41	[12]
Silica	3.03	[72]
Bentonite	33.78	[73]
Coconut shell activated carbon	51.56	[74]
Acid activated pine sawdust (APSD)	312.50	Present study

utilized in modeling the adsorption data.

The R-P isotherm represents an empirical isotherm that contains three parameters and is a mix of the Langmuir and Freundlich isotherms. Thus, the adsorption mechanism represents a mixture, and ideal monolayer adsorption is not followed. It has two restricting behaviors: when β=1, the Langmuir form, and when β=0, Henry's law. Furthermore, if β is in the range of 0-1, it shows favorable adsorption [65]. Table 4 demonstrates the R-P isotherm constants for the dye adsorption onto APSD. As the exponent, adsorption is in the Langmuir form as β tends to 1.

According to the evaluation of the coefficients obtained for the isotherms (Table 4), the adsorption process conformed to the Langmuir isotherm, so that the physical adsorption mechanism was applied. The adsorption process was favorable, and the adsorption was good. Furthermore, the comparison of the values of the maximum adsorption capacity acquired from the present research with values obtained from other specified adsorbents is significant because this will indicate the efficiency of APSD as a possible adsorbent to treat water that contains MR GRL dye. A list that demonstrates the adsorption capacity of various materials for the sorption of MR GRL from their aqueous solutions is presented in Table 5. As observed there, the adsorption capacity of APSD for MR GRL adsorption was quite good in proportion to other inexpensive adsorbents.

6. Thermodynamic Parameters

Thermodynamic parameters, such as alteration in the standard Gibbs free energy (ΔG^o), enthalpy (ΔH^o), and entropy (ΔS^o) of adsorption, were found by means of the equations presented below:

$$\Delta G^o = -RT \ln K_c \quad (7)$$

$$Kc = q_e/C_e \quad (8)$$

$$\Delta G^o = \Delta H^o - T\,\Delta S^o \quad (9)$$

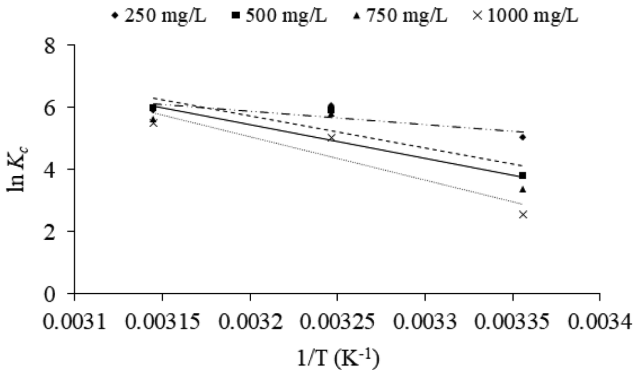

Fig. 12. van't Hoff Plot for adsorption of MR GRL dye onto APSD.

$$\ln K_c = \frac{\Delta S^o}{R} - \frac{\Delta H^o}{RT} \quad (10)$$

where K_c denotes the distribution coefficient of the adsorbate, q_e and C_e denote the equilibrium dye concentration on APSD (mg/g) and in the solution (mg/L), respectively. T refers to the temperature (K), and R refers to the universal gas constant (8.314 J/mol K). It is possible to compute ΔH^o and ΔS^o parameters from the slope and intercept of the plot $\ln K_c$ vs. 1/T, respectively (Fig. 12). The results are shown in Table 6.

Negative values of free energy change (ΔG^o) (Table 6) suggest that adsorption occurs spontaneously, whereas there is no need for an energy input from outside of the system, and adsorption is favorable in the range of the studied temperatures. The increasing negative value of ΔG^o along with the increasing temperature shows that adsorption takes place more spontaneously at higher temperatures.

The positive value of ΔS^o proves the increase in randomness at the interface between the solid and liquid in the course of adsorp-

Table 6. Thermodynamic parameters

	ΔG^o (kJ/mol)			ΔH^o (kJ/mol)	ΔS^o (kJ/mol·K)
C_o (mg/L)	298 K	308 K	318 K		
250	−84.489	−86.122	−87.756	−35.797	0.163
500	−184.736	−188.006	−191.276	−87.280	0.327
750	−190.125	−193.472	−196.818	−90.398	0.335
1000	−239.755	−243.898	−248.040	−116.313	0.414

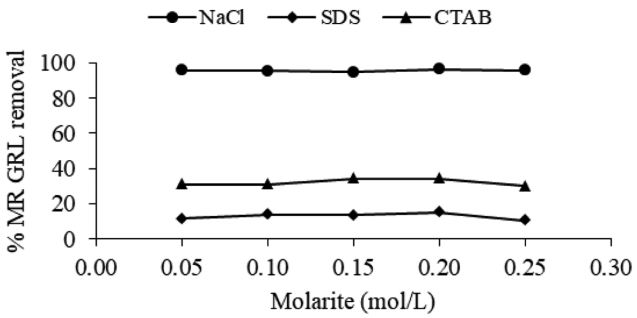

Fig. 13. Influence of ionic strength on efficiency.

tion, and it can also point to ion exchange reactions forming steric hindrance. Moreover, it can demonstrate that great hydrated dye anions release water molecules in the course of adsorption [75]. The enthalpy change (ΔH^o) because of chemisorption is positive in the range of 40-120 kJ/mol [76]. Therefore, negative values of ΔH^o for the MR GRL adsorption acquired in the current research showed that adsorption occurred probably because of physisorption. The negative value of ΔH^o, as demonstrated in Table 6, reflected the exothermic character of adsorption.

7. Impact of Ionic Strength

Colored wastewater includes many inorganic salts that can affect the dye sorption. Surfactants are frequently found in dye-containing industrial wastewaters. Therefore, the effect of surfactants and salts on the removal of cationic dye (MR GRL) used in the study must be investigated. Therefore, the impact of inorganic salt and surfactants such as NaCl, SDS, CTAB at a concentration of 0.05-0.25 mol/L on the adsorption process of MR GRL by APSD, was investigated (Fig. 13).

Fig. 13 shows that the effect of NaCl salt on the dye removal efficiency is hardly ever possible. However, studies were also conducted with two different surfactants, anionic and cationic, such as sodium dodecyl sulfate (SDS) and cetyltrimethylammonium bromide (CTAB), respectively. As shown in Fig. 13, when SDS and CTAB were added, the increased ionic charge of the solution caused the decreased adsorption percentage of the dye. Nevertheless, the increase in the concentrations of NaCl, SDS, and CTAB did not cause any additional negativity on the dye removal efficiency. These findings demonstrate that electrostatic attraction is crucial to removing MR GRL. The reason for the above-mentioned situation may be the decreased affinity of dye molecules and sorption zones. If electrostatic attraction represents the major mechanism of adsorption, ionic strength has a considerable adverse impact on the adsorption process [47]. The effect of NaCl concentration on adsorption of MB/MG on PSP/PLP was studied by Gupta [77]. As the ionic strength increased, the effective concentration of MB and MG decreased; therefore, the adsorptive capacity of dyes onto adsorbents decreased. Other studies [39,78-80] with modified ionic strength were found to be strongly dependent on ionic strength, indicating an ion exchange mechanism.

CONCLUSIONS

Acid-activated pine sawdust was used as an adsorbent for disposal of MR GRL from the aqueous solution. SEM, EDX, and FTIR analyses were conducted to characterize the activated pine sawdust, and the following conclusions were reached:

a. The maximum percentage removal of 99.35%, 99%, and 69.44% was achieved at a dye concentration of 250 mg/L using APSD, BPSD, and PSD, respectively, as the adsorbents, confirming the high efficiency of applying APSD in MR GRL removal. Chemical reagents could increase BET surface area, pore volume and especially surface functional groups that enhance the adsorption of material. The results showed that the MR GRL adsorption capacity was positively correlated to the BET surface area. The H_2SO_4 treated PSD (APSD) adsorbent had greater BET surface area (19.11 m^2/g) and more active sites for MR GRL adsorption from aqueous solution.

b. Five adsorption isotherm models were analyzed in the current study, and the removal of MR GRL on APSD fitted well to the Langmuir, isotherm model for the equilibrium data.

c. A pseudo-second-order reaction rate was followed by the kinetics of MR GRL sorption using APSD.

d. The adsorption experiments for different temperatures in this study detected the exothermic nature and spontaneous character of the adsorption process. It also implies that the diffusion process does not dominate adsorption.

The obtained findings show the great potential of the studied adsorbent as an effective sorbent to remove MR GRL from wastewater, which would otherwise be discarded in landfills or used as a fuel in boilers for energy production.

As real textile wastewater contains more than one pollutant, the presence of other pollutants may interfere with the removal efficiency of an individual one. As a result, the effect of coexisting pollutants should be addressed when conducting an adsorption study. For this reason, this study for color removal from synthetic textile wastewater should be tested in real textile wastewater and the removal efficiency of other parameters should be investigated besides color removal.

CONFLICT OF INTEREST

As the author(s), we declare that there is no conflict of interest regarding the publication of this article.

ACKNOWLEDGEMENT

We would like to thank Prof. Dr. Ayten ATEŞ from Sivas Cumhuriyet University for Brunauer-Emmett-Teller (BET) surface area analysis.

REFERENCES

1. M. T. Yagub, T. K. Sen, S. Afroze and H. M. Ang, *Adv. Colloid Interface Sci.*, **209**, 172 (2014).
2. S. Benhabiles and K. Rida, *Part. Sci. Technol.*, In Press (2020).
3. S. Arslan, M. Eyvaz, E. Gürbulak and E. Yüksel, in *Textile wastewater treatment*, E. A. Kumbasar Ed., IntechOpen Limited, London (2016).
4. G. O. El-Sayed, T. Y. Mohammed and A. A.-A. Salama, *ISRN Environ. Chem.*, **2013**, 1 (2013).

5. R. Javaid and U. Y. Qazi, *Int. J. Environ. Res. Public. Health*, **16**, 2066 (2019).
6. N. Thinakaran, P. Baskaralingam, M. Pulikesi, P. Panneerselvam and S. Sivanesan, *J. Hazard. Mater.*, **151**, 316 (2008).
7. M. Doğan, M. H. Karaoğlu and M. Alkan, *J. Hazard. Mater.*, **165**, 1142 (2009).
8. P. Vijayalakshmi, V. S. S. Bala, K. V. Thiruvengadaravi, P. Panneerselvam, M. Palanichamy and S. Sivanesan, *Sep. Sci. Technol.*, **46**, 155 (2011).
9. G. El-Sayed, *Int. Res. J. Pure Appl. Chem.*, **4**, 402 (2014).
10. G. T. Canbaz, N. K. Çakmak, A. Eroğlu and Ü. Açıkel, *Int. Adv. Res. Eng. J.*, **3**, 75 (2019).
11. M. H. Karaoğlu, M. Doğan and M. Alkan, *Micropor. Mesopor. Mater.*, **122**, 20 (2009).
12. F. Deniz, *Environ. Prog. Sustain. Energy*, **33**, 396 (2014).
13. Md. A. Islam, I. Ali, S. M. A. Karim, Md. S. Hossain Firoz, A.-N. Chowdhury, D. W. Morton and M. J. Angove, *J. Water Process Eng.*, **32**, 100911 (2019).
14. P. K. Malik, *J. Hazard. Mater.*, **113**, 81 (2004).
15. F. Mehrabi, A. Vafaei, M. Ghaedi, A. M. Ghaedi, E. Alipanahpour Dil and A. Asfaram, *Ultrason. Sonochem.*, **38**, 672 (2017).
16. M. A. M. Salleh, D. K. Mahmoud, W. A. W. A. Karim and A. Idris, *Desalination*, **280**, 1 (2011).
17. S. N. Jain and P. R. Gogate, *J. Mol. Liq.*, **243**, 132 (2017).
18. F. Deniz and R. A. Kepekci, *Microchem. J.*, **132**, 172 (2017).
19. S. M. Yakout, M. R. Hassan, M. E. El-Zaidy, O. H. Shair and A. M. Salih, **14**(2), 4560 (2019).
20. V. Dulman and S. M. Cucu-Man, *J. Hazard. Mater.*, **162**, 1457 (2009).
21. M. Özacar and İ. A. Şengil, *Bioresour. Technol.*, **96**, 791 (2005).
22. F. Batzias and D. Sidiras, *J. Hazard. Mater.*, **114**, 167 (2004).
23. V. K. Garg, R. Gupta, A. Bala Yadav and R. Kumar, *Bioresour. Technol.*, **89**, 121 (2003).
24. A. E. Ofomaja, *Chem. Eng. J.*, **143**, 85 (2008).
25. S. Akhouairi, H. Ouachtak, A. A. Addi, A. Jada and J. Douch, *Water. Air. Soil Pollut.*, **230**, 181 (2019).
26. F. Ferrero, *J. Hazard. Mater.*, **142**, 144 (2007).
27. O. Hamdaoui, *J. Hazard. Mater.*, **135**, 264 (2006).
28. J. J. Salazar-Rabago, R. Leyva-Ramos, J. Rivera-Utrilla, R. Ocampo-Perez and F. J. Cerino-Cordova, *Sustain. Environ. Res.*, **27**, 32 (2017).
29. A. A. Azzaz, S. Jellali, R. Souissi, K. Ergaieg and L. Bousselmi, *Environ. Sci. Pollut. Res.*, **24**, 18240 (2017).
30. M. Rafatullah, O. Sulaiman, R. Hashim and A. Ahmad, *J. Hazard. Mater.*, **177**, 70 (2010).
31. M. S. U. Rehman, I. Kim and J.-I. Han, *Carbohydr. Polym.*, **90**, 1314 (2012).
32. İ. Şentürk and M. Alzein, *Acta Chim. Slov.*, **67**, 15 (2020).
33. M. A. K. M. Hanafiah, W. S. W. Ngah, S. H. Zolkafly, L. C. Teong and Z. A. A. Majid, *J. Environ. Sci.*, **24**, 261 (2012).
34. A. Ates, A. Reitzmann, C. Hardacre and H. Yalcin, *Appl. Catal. Gen.*, **407**, 67 (2011).
35. M. A. Ferro-García, J. Rivera-Utrilla, I. Bautista-Toledo and C. Moreno-Castilla, *Langmuir*, **14**, 1880 (1998).
36. K. Kuśmierek and A. Świątkowski, *Pol. J. Chem. Technol.*, **17**, 23 (2015).
37. T. K. Trinh and L.-S. Kang, *Environ. Eng. Res.*, **15**, 63 (2010).
38. K. Y. Foo and B. H. Hameed, *Bioresour. Technol.*, **111**, 425 (2012).
39. K. Gul, S. Sohni, M. Waqar, F. Ahmad, N. A. N. Norulaini and A. K. M. Omar, *Carbohydr. Polym.*, **152**, 520 (2016).
40. B. M. Babić, S. K. Milonjić, M. J. Polovina and B. V. Kaludierović, *Carbon*, **37**, 477 (1999).
41. Z. Movasaghi, B. Yan and C. Niu, *Ind. Crops Prod.*, **127**, 237 (2019).
42. D. Sidiras, F. Batzias, E. Schroeder, R. Ranjan and M. Tsapatsis, *Chem. Eng. J.*, **171**, 883 (2011).
43. J. Lykiema, K. S. W. Sing, J. Haber, M. Kerker, E. Wolfram, J. H. Block, N. V. Churaev, D. H. Everett, R. S. Hansen, R. A. W. Haul, J. W. Hightower and R. J. Hunter, *Pure Appl. Chem.*, **57**(4), 603 (1985).
44. A. Ma and M. Mm, *J. Chromatogr. Sep. Technol.*, **7**, 1 (2016).
45. R. Thenmozhi and T. Santhi, *Int. J. Environ. Sci. Technol.*, **12**, 1677 (2015).
46. P. Yang, Y. Xu, J. Tuo, A. Li, L. Liu and H. Shi, *R. Soc. Open Sci.*, **6**, 181986 (2019).
47. R. Lafi and A. Hafiane, *J. Taiwan Inst. Chem. Eng.*, **58**, 424 (2016).
48. F. Deniz and R. A. Kepekci, *J. Mol. Liq.*, **219**, 194 (2016).
49. A. G. El-Said, *J. Am. Sci.*, **6**, 143 (2010).
50. W. S. Wan Ngah and M. A. K. M. Hanafiah, *BioChemEng. J.*, **39**, 521 (2008).
51. G. Moussavi and B. Barikbin, *Chem. Eng. J.*, **162**, 893 (2010).
52. C. Xiaoli and Z. Youcai, *J. Hazard. Mater.*, **137**, 410 (2006).
53. A. Kuleyin and F. Aydin, *Environ. Prog. Sustain. Energy*, **30**, 141 (2011).
54. K. G. Akpomie, F. A. Dawodu and K. O. Adebowale, *Alexandria Eng. J.*, **54**(3), 757 (2015).
55. S. K. Nadavala, K. Swayampakula, V. M. Boddu and K. Abburi, *J. Hazard. Mater.*, **162**, 482 (2009).
56. I. A. W. Tan, A. L. Ahmad and B. H. Hameed, *J. Hazard. Mater.*, **154**, 337 (2008).
57. Z. Rawajfih and N. Nsour, *J. Colloid Interface Sci.*, **298**, 39 (2006).
58. N. Ali, P. Pal, F. Banat and C. Srinivasakannan, *Sep. Sci. Technol.*, **54**, 2671 (2019).
59. F. Togue Kamga, *Appl. Water Sci.*, **9**, 1 (2019).
60. A. O. Dada, A. P. Olalekan, A. M. Olatunya and O. Dada, *IOSR J. Appl. Chem.*, **3**, 38 (2012).
61. K. Y. Foo and B. H. Hameed, *Chem. Eng. J.*, **156**, 2 (2010).
62. T. P. K. Murthy, B. S. Gowrishankar, M. N. C. Prabha, M. Kruthi and R. H. Krishna, *Microchem. J.*, **146**, 192 (2019).
63. B. E. Reed and M. R. Matsumoto, *Sep. Sci. Technol.*, **28**, 2179 (1993).
64. H. A. Akalin, Ü. Hiçsönmez and H. Yılmaz, *J. Turk. Chem. Soc. Sect. Chem.*, **5**(1), 85 (2018).
65. N. Ayawei, A. N. Ebelegi and D. Wankasi, *J. Chem.*, **2017**, 1 (2017).
66. Y. Gao, Y. Li, L. Zhang, H. Huang, J. Hu, S. M. Shah and X. Su, *J. Colloid Interface Sci.*, **368**, 540 (2012).
67. K. V Kumar and S. Sivanesan, *Dyes Pigm.*, **72**, 124 (2007).
68. H. Rezania, V. Vatanpour, E. Salehi, N. Gavari, A. Shockravi and M. Ehsani, *J. Polym. Environ.*, **27**, 1790 (2019).
69. F. Çiner, *Glob. NEST J.*, **20**, 1 (2017).
70. M. Sarioglu Cebeci and M. Aşkal, *Glob. NEST J.*, **20**, 25 (2017).
71. H. Irinislimane and N. Belhaneche-Bensemra, *Chem. Eng. Commun.*, **204**, 897 (2017).
72. M. Koyuncu, *Orient. J. Chem.*, **25**(1), 35 (2009).
73. M. Koyuncu, *Asian J. Chem.*, **21**, 5458 (2009).
74. A. M. Aljeboree, A. N. Alshirifi and A. F. Alkaim, *Arab. J. Chem.*,

10, 3381 (2017).
75. A. Witek-Krowiak, *Chem. Eng. J.*, **171**, 976 (2011).
76. M. Alkan, Ö. Demirbaş, S. Çelikçapa and M. Doğan, *J. Hazard. Mater.*, **116**, 135 (2004).
77. N. Gupta, A. K. Kushwaha and M. C. Chattopadhyaya, *Arab. J. Chem.*, **9**, 707 (2016).
78. M. A. Khan, Z. A. A. Othman, M. Kumar, M. S. Ola and M. R. Siddique, *Desalination Water Treat.*, **56**, 146 (2015).
79. R. Gong, Y. Sun, J. Chen, H. Liu and C. Yang, *Dyes Pigm.*, **67**, 175 (2005).
80. H. El Boujaady, M. Mourabet, A. El Rhilassi, M. Bennani-Ziatni, R. El Hamri and A. Taitai, *J. Saudi Chem. Soc.*, **21**, 94 (2017).